Dynamic arrays based on magnetically controlled Fe3O4 particles

Ivan Shorstkii*

Kuban State University of Technology, Department of Technological equipment and life-support systems, Krasnaya Street 135, Krasnodar, Russian Federation

Abstract. In this work, a new concept of dynamic granular arrays was proposed based on magnetically controlled particles. Method of external rotating magnetic field (ERMF), based on a dipole interaction of magnetic spherical Fe_3O_4 particles in highly ordered volume arrays is proposed. The microwave-absorbing characteristics results of developed composites offer an effective way to design high-performance functional materials to facilitate the research in electromagnetic shielding and microwave absorption.

1 Introduction

Arising from the rapid development of electronic devices, wireless communication tools, and local area networks, electromagnetic interference (EMI) has greatly threatened human health and disturbed various commercial or industrial equipment [1−2]. Thus, the demand for electromagnetic absorbents has become urgent over the past years. It is well-known that an electromagnetic absorbent is a type of functional material that is able to absorb incidence of electromagnetic wave effectively and then convert it into thermal energy. The ideal absorbing materials must have light weight, strong absorption, thin thickness, and broad frequency. Several factors, such as morphology, geometry, and microstructure, are crucial in determining the electromagnetic absorption properties. Currently, different morphologies of absorbents have been fabricated by various methods, containing one dimensional (1D; nanowires, nanoparticles), two-dimensional (2D; flake, nanodisks) and three-dimensional (3D; tubes, sphere, urchin-like structure) [3−5].

In this study, a novel method was designed for porous 3D granular arrays fabrication based on magnetically controlled particles as a new type of microwave absorption materials. These well-defined structures consist of numerous air pores. At the same time, the porous structure with a lower density can be used as lightweight microwave absorption material. Method of external rotating magnetic field (ERMF), based on a dipole interaction of magnetic spherical Fe_3O_4 particles in highly ordered volume arrays is proposed to form the array of particles. When magnetic particles are placed inside the ERMF the particles are aligned along the field lines of the dipole field and are entrained in its displacement [6]. On the basis of this principle, a technique is developed for the formation of dynamic flat and 3-D particles arrays with a given packing structure.

*Corresponding author: thegector@mail.ru

2 Experimental section

Fe_3O_4 microparticles were purchased from Ricoh Company (Japan). Particles composition were determined by X-ray phase analysis (XRD) on a Shimadzu XRD-7000 S diffractometer (Japan).

The 3-D composite was of dynamic arrays prepared using external rotating magnetic field effect on lab setup (Figure 1). Experimental lab setup consists of a platform, cylindrical tube, nozzle with permanent magnets and two stepper motors with a control panel.

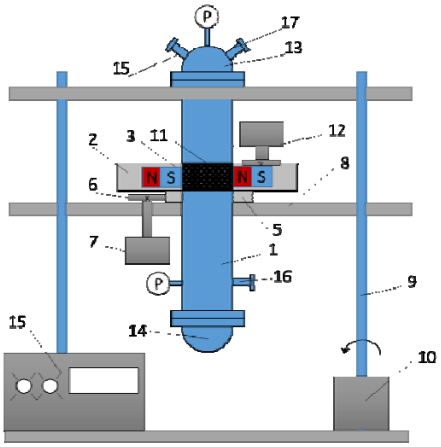

Fig. 1. ERMF lab setup.

On the outside of the tube, 1 is a cylindrical nozzle 2 with diametrically opposed two permanent magnets 3 disposed of therein and a mechanical pole switcher 12. The cylindrical nozzle has a gear train 5 through which it is connected to a gear 6 connected to an electric motor 7, mounted on a reciprocating platform 8 by means of a pin 9 controlled by an electric motor 10. Inside the tube, there are Fe_3O_4 particles 11. The housing comprises a lid dressing array of particles 13 and the discharge cover 14 to remove composite from the tube. The control of the electric motors is carried out using the control panel 15. Neodymium magnets create an external rotating magnetic field around the tube and fixed in the nozzle and close contact with a glass tube.

Particles placed inside the tube and captured by the magnetic field of permanent magnets 3. Cylindrical nozzle 2 starts rotating and reconstructing particles from the fibrous dispersed into a dense package, forming particles array [7]. To obtain a composite material and study reflection spectrum and the frequency characteristics of attenuation of electromagnetic radiation, paraffin was added to the medium of the particle array in a volume ratio of 1:1. This composition was brought to the melting point of the paraffin with an alcohol burner. After a homogeneous mass was obtained, the tube was moved to the zone of the magnetic packing by means of a reciprocating platform. Permanent magnets provided the creation of an external rotating magnetic field around the tube, to form dynamic particles arrays. After the paraffin had solidified, the composite was removed. Then the compact sample was cut into parallelepiped with 23x10x3 mm size. During samples preparation, the length of samples was fit with the direction of magnetic field.

Sample with flat arrays was prepared by pressing a sticky tape against particles and reciprocating translational motion of magnetic dipole along the plane of a sticky tape, then place another sticky tape for sealing. To study individual particles, particles were separated by a needle and placed on sticky tape, forming dispersed arrays. As an extension to current research, samples with larger inter-array distance were made.

A time-varying magnetic field was used to magnetize the samples on Vibrating Sample Magnetometry (VSM, IMRE, and Singapore). Furthermore, the vibrating sample holder is secured on a rotation stage that allows variation of φ between 0° and 90° in order to analyze magnetization of the sample at different azimuth angle φ between external field and sample plane.

The composition and phase purity of samples were analyzed by X-ray diffraction (XRD) at 40 kV voltage and 30 mA current with CuKα radiation (l = 1.541 Å). Scanning electron microscopy (SEM) images were obtained on a JEOL JSM 6300 scanning electron microscope at an acceleration voltage of 15 kV.

The microwave-absorbing characteristics were evaluated by measuring the reflection loss using a P2-61 scalar quantity network analyzer in the 8-12 GHz band range. All the measurements were performed at room temperature.

The RL coefficient curves were calculated from the relative permeability and permittivity for a given frequency and absorber thickness, according to the following equations:

$$RL(dB) = 20\ log\ |(Z_{in}-Z_0)/(Z_{in}+Z_0)| \quad (1)$$

Where the Z_0 - the impedance of free space and Z_{in} - the input impedance of the absorber.

3 Results and discussion

Figure 2 shows the XRD pattern of samples. Analyzing the X-ray diffraction pattern of the investigated particle samples, it shows a significant part of the substance is in the x-ray morphological state. When compared to the PDF-2 and PDF-4 database, the material under investigation was identified as Iron Oxide (Fe_3O_4).

When the process of rotation of the nozzle with permanent magnets around the cylindrical tube occurs, the spherical particles Fe_3O_4 are densified with a uniform distribution of the particle density in the 3D of the array (Figure 2). A transition occurs from the dispersed fibrous structure of spherical particles to a dense package with a porosity ε = 0.259 close to the porosity of a face-centered package.

Figure 2 is a low magnification SEM image showing a group of Fe_3O_4 particles. These particles are nearly spherical in shape with a narrow diameter distribution of around 50–60 μm. The SEM image, as shown in figure 2, clearly indicates that all the particles own a ‘core/shell' type microstructure and the inner Fe cores , into the ‘onion' type carbon cages. The formed volume array of microspherical particles has a porous channel structure with pores of approximately 15 μm in diameter.

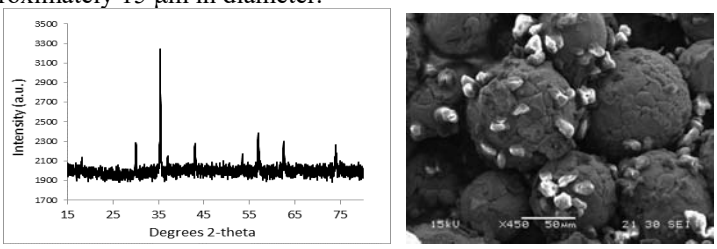

Fig. 2. XRD patterns (left) and SEM images of 3-D particles arrays (right).

Magnetic anisotropy was more clearly observed in compact arrays—the dependence of parallel and perpendicular magnetization on the direction of the applied field with respect to the sample plane samples reach saturation slower and at the higher field as φ increases. Since a smaller distance between adjacent particles would entail interaction, was reasonable to postulate that interaction between particles may result in the anisotropy observed.

Moreover, at the same φ, compact samples reach saturation faster than dispersed samples. Thus, if interaction does exist, it would most likely have the intensifying effect on the external field. The hypothesis can only be tested out through modeling of the interaction in compact array case within mean field approximation and compare it with the experimental data. However, the magnetic moment density of the particles is required for applying mean field approximation and it can only be obtained from the dispersed arrays. As a result, dispersed arrays of both shapes were first modeled to facilitate the modeling of interaction field in compact arrays.

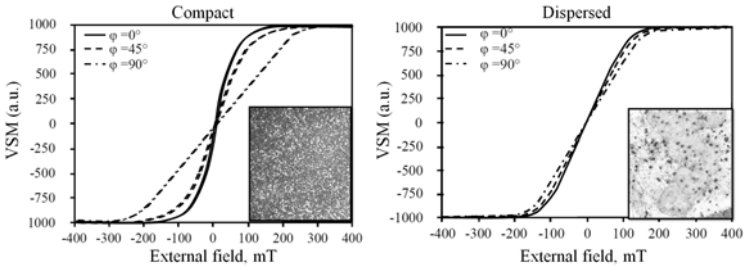

Fig. 3. Magnetization curves for compact and dispersed packaging at azimuth 0°, 45° and 90°.

For 2D arrangement where particles were dispersed by a distance of more than 10 times of their radius, interaction among particles was minimized. Thus, the entire 2D plane can be modeled by considering a single particle due to the relative uniformity of particle size. When external magnetic field is applied, randomly arranged atomic dipoles inside the particle slowly align with the external field. Due to isotropic property of spherical particle and the absence of magnetic dipole interaction among particles, the total magnetization of the selected particle is always parallel or antiparallel to the external field. The process of magnetization can be modeled by a domain wall with zero width that sweeps through the particle to increase the number of dipoles that align with the external field. As a reasonable simplification, particles are assumed to be cubic in shape and the domain wall is parallel to both external field and two sides of the cube.

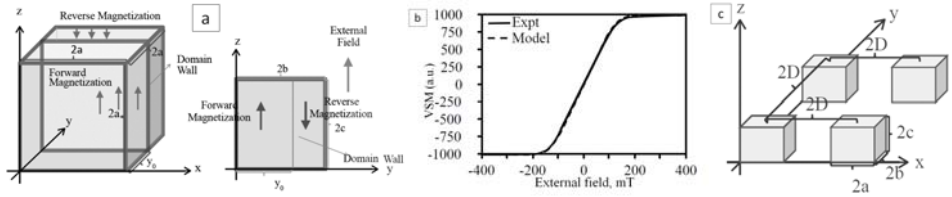

Fig. 4. Schematic of domain wall position (a), the comparison between model and experiment (b), and schematic of arrays on sample plane (c).

At any external field, the domain wall position always minimizes the Zeeman Energy of the selected particle, which is the potential energy of the magnetized particle in an external magnetic field. By equating the first derivative of energy with respect to domain wall position to be zero, the expression of the domain wall position at any external field before saturation is found to be $y_0 = b + \pi B_{ext}\alpha / \mu_0 M$. With domain wall position determined and the magnetization of the sample in terms of the external magnetic field expressed. The sample reaches saturation when y = a. Thus, the corner field at which the sample saturates is $B_{cor} = \mu_0 M / \pi$. After saturation, the magnetization of the particle remains constant. By comparing the model curve and the experimental curve (Figure 4) was found that our model is capable of accurately predicting the saturation rate and saturation point for a 2D dispersed sample with spherical particles. Saturation magnetization is reached at around 120mT and the magnetic moment density is found to be around 3040 A/m.

Particles in the compact sample are suspected to interact with each other. The expression of the interaction field can be derived with mean field approximation. A point at the edge of a semi-infinite plane is chosen and the field from surrounding particles is doubly integrated into polar coordinate from zero to infinity and zero to 2π. The distance between particles was first assumed to be zero for simplification purpose and was account for later by a parameter a^2/d^2 representing the density of the sample (Figure 4).

After saturation, a further increment of the external field will not result in changes in the magnitude but a change in direction of total magnetization. This is because the alignment of magnetization direction with external field direction minimizes the energy of the sample.

To further reveal the microwave absorption properties of the Fe_3O_4 composites, the reflection loss R was analyzed by comparing known literature data of Fe_3O_4 particles [8-10] and obtained experimental data. A comparison of the reflection coefficient data presented as spectra is shown in Figure 5. The maximum value of RL was obtained for a sample of a 3 mm thick volume array at a frequency of 12 GHz and corresponded to 3.5 dB. Increasing the thickness of the sample leads to an increase in the reflection coefficient. From the comparative analysis, it can be seen that the formed structure of densely packed particles has better electromagnetic fields protection properties in comparison with chaotically ordered particles.

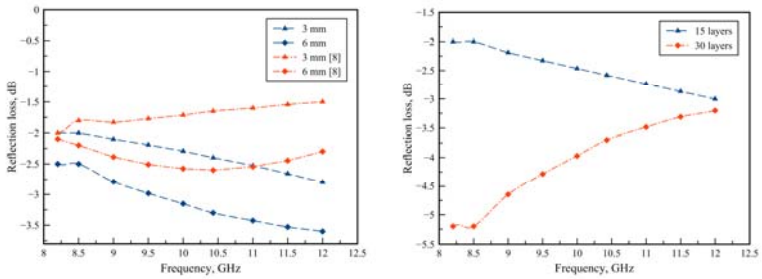

Fig. 5. Microwave reflection loss RL of Fe_3O_4 arrays particles–paraffin wax sample versus frequency and layer of flat arrays.

The results of measuring the reflection loss for samples of flat arrays differing in the number of layers are shown in Figure 5. The maximum RL value -5.2 dB fixed at a frequency of 8.5 GHz. Unlike the spectra of 3D arrays, increasing the layers of flat arrays leads to a decrease in the reflection coefficient because of partial energy loss of electromagnetic radiation in interaction with a flat 2D array depends on the dipole-dipole interaction and the surface density of Fe_3O_4 composite.

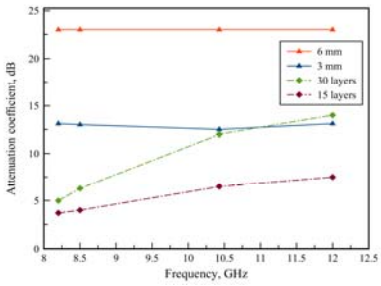

Fig. 6. Attenuation coefficient of Fe_3O_4 arrays particles–paraffin wax sample and layer of flat arrays versus frequency.

3D samples thickness leads to double increase EMR attenuation coefficient from 13 dB for 3 mm sample up to 24 dB for a 6 mm sample in 8...12 GHz range. The increase of the

thickness of the samples of flat arrays leads to double decrease the EMR attenuation coefficient from 14 dB for a sample with 15 flat layers based on Fe_3O_4 particles up to 7 dB for the sample in with 30 layers at 12 GHz frequency.

4 Conclusion

The method of rotating the magnetic field of dipoles and the installation for its realization have shown the possibility of forming dynamic 3-D arrays of spherical particles with porosity $\varepsilon = 0.259$. Composite material obtained by this method has a small coercive force and a small residual magnetization, which affects the reflection spectra of the electromagnetic radiation. The magnetic susceptibility of the claimed composite material depends on the physical nature of the particles of the Fe_3O_4 material and on its geometric shape. The interaction between particles in compact arrays has been modeled within mean field approximation. Fitting to our data shows that the interactions between particles were found to be in good agreement with the average distance between particles. Part of the energy of electromagnetic radiation when interacting with this material is dissipated to overcome the demagnetizing factor associated with geometric parameters and to overcome the magnetic susceptibility associated with the nature of the material. Thus, the partial loss of the energy of electromagnetic radiation in interaction with a flat 2D array depends on the dipole-dipole interaction and the surface density of the Fe_3O_4 composite.
By using a rotational magnetic field of dipoles based on nano and microparticles interactions, it is possible to create types of microwave absorptive materials in a wide frequency range while maintaining strong absorption that has mechanical strength, manufacturability with usability.

References

1. H. Lv, X. Liang, G. Ji, H. Zhang, Y. Du. ACS applied materials & interfaces, **18**, 9776 (2015)
2. F. Li, J. Wu, Q. Qin, Z. Li, X. Huang. Powder Technology, **2**, 267 (2010)
3. Y. Li, K. Pan, G. Wang, N. Fan, X. Miao. Journal of Materials Research, **22**, 2867, (2011)
4. Q. Liu, Q. Cao, H. Bi, C. Liang, K. Yuan, W. She, R. Che, Q. Liu. Advanced Materials, **3**, 486, (2016)
5. X.F. Zhang, X.L. Dong, H. Huang, B. Lv, J.P. Lei, C.J. Choi. J. of Physics D: App. Ph., **7**, 5383, (2017)
6. Y.H. Li, C.Y. Chen, S.T. Sheu, J.M. Pai. Microfluidics and nanofluidics, **4**, 579, (2012)
7. I.A. Shorstkii, K.Yu. Savenkov. Sci. J. NRU ITMO. Processes and Food Production Equipment, **4**, 20, (2017)
8. X. Jian, B. Wu, Y. Wei, S.X. Dou, X. Wang, W. He, N. Mahmood. ACS applied materials & interfaces, **9**, 6101, (2016)
9. Y. Du, W. Liu, R. Qiang, Y. Wang, X. Han, J. Ma, P. Xu. ACS applied materials & interfaces, **15**, 12997, (2014)
10. Y. Hou, H. Yuan, H. Chen, J. Shen, L. Li. Science China Chemistry, **6**, 740, (2017)